Biochemical Pharmacology, Vol. 56, pp. 1209–1217, 1998.

ISSN 0006-2952/98/$19.00 + 0.00
PII S0006-2952(98)00255-X

Kinetics of Anthracycline Accumulation in Multidrug-resistant Tumor Cells: Relationship to Drug Lipophilicity and Serum Albumin Binding

Erland J. F. Demant† and Ellen Friche‡*

†Department of Medical Biochemistry and Genetics, Biochemistry Laboratory C, The Panum Institute, University of Copenhagen, 2200 Copenhagen N, Denmark; and ‡Department of Hematology, The Finsen Center, Rigshospitalet, 2100 Copenhagen Ø, Denmark

ABSTRACT. A multidrug-resistant Ehrlich ascites tumor cell line (EHR2/DNR+) was used to examine the membrane transport kinetics of lipophilic anthracycline derivatives in the presence of serum albumin. We present a model for theoretical data analysis with consideration of drug–albumin complex formation. For a set of five derivatives (doxorubicin, daunorubicin, 4-demethoxydaunorubicin, 4′-deoxy-4′-iododoxorubicin, and 13-dihydro-4′-deoxy-4′-iododoxorubicin), data were given on the rates of diffusional drug uptake, and membrane permeability coefficients of the noncharged molecules were estimated. Both the initial rates and the steady-state levels of drug uptake were found to decrease by addition of BSA at concentrations ranging from 5 to 75 mg/mL. For each drug, this effect of serum albumin could be accounted for by the altered distribution between free and protein-bound drug molecules in the bulk aqueous medium. A good fit of theoretical accumulation curves to the experimental data was obtained. It was concluded that a mathematical simulation method makes it possible to predict the uptake characteristics of lipophilic anthracycline compounds into tumor cells under serum conditions. BIOCHEM PHARMACOL **56**;9:1209–1217, 1998. © 1998 Elsevier Science Inc.

KEY WORDS. anthracyclines; transport kinetics; multidrug resistance (MDR); serum albumin; lipophilicity; P-glycoprotein

One of the best-characterized MDR§ mechanisms is associated with the ATP-dependent membrane transporter Pgp [1, 2]. Kinetic studies in experimental cell culture systems indicate that Pgp functions to efflux hydrophobic and cytotoxic drugs across cell membranes [1, 3–5], thereby lowering the intracellular drug concentration to nontoxic levels. Substrates for the efflux transporter in MDR tumor cells include the clinically important anthracyclines daunorubicin and doxorubicin [6]. A large number of derivatives have therefore been examined in structure–activity relationship studies with the purpose of identifying new compounds that are able to overcome the efflux system. Derivatives which appear promising are generally more lipophilic and have a higher membrane permeability than the parent compounds [7–10]. 4-Demethoxydaunorubicin [11] and 4′-deoxy-4′-iododoxorubicin [12] provide two important examples. As the lipophilic character of the anthracyclines is increased by modifying their molecular structure, the extent of protein binding to extracellular components such as serum albumin is increased as well [13–16]. Therefore, without consideration of anthracycline-albumin complex formation, *in vitro* test systems may not be useful in predicting transport and biological properties that are clinically relevant. Kinetic studies on the cellular accumulation of lipophilic anthracyclines were performed in our laboratory using the Ehrlich ascites MDR tumor cell line EHR2/DNR+ under medium conditions with bovine serum at concentrations up to 5% [17, 18]. This work is now extended to include an analysis of the influence of a range of serum albumin concentrations on the uptake process for anthracyclines with varying lipophilicity: doxorubicin (**1**), daunorubicin (**2**), 4-demethoxydaunorubicin (**3**), 4′-deoxy-4′-iododoxorubicin (**4**), and 13-dihydro-4′-deoxy-4′-iododoxorubicin (**5**) (Fig. 1). By using experimental data on drug membrane permeability and binding affinity for BSA in a mathematical model for computer simulations [19], we have attempted to predict the time-courses for drug uptake at physiologically relevant albumin concentrations.

* Corresponding author: Dr. Erland J. F. Demant, Department of Medical Biochemistry & Genetics, Biochemistry Laboratory C, The Panum Institute, University of Copenhagen, Blegdamsvej 3, DK-2200 Copenhagen N, Denmark. Tel. (45) 35 32 77 97; FAX (45) 35 36 79 80.

§ *Abbreviations:* A_{st}, steady-state level of anthracycline; BCECF-AM, 2′,7′-bis(2-carboxyethyl)-5(6)-carboxyfluorescein-triacetoxymethyl ester; [BSA], concentration of bovine serum albumin; D_{lipid}, diffusion coefficient within the membrane lipid phase; FITC, fluorescein isothiocyanate; J_{12}, unidirectional influx; $J_{21,P}$, glucose-dependent efflux; K_{lipid}, K_{DNA}, and K_{BSA}, anthracycline binding constants to lipid, DNA, and BSA, respectively; MDR, multidrug resistance; Pgp, P-glycoprotein; P_{ow}, 1-octanol/buffer partition coefficient; P_{plas}, permeability coefficient of the plasma membrane to the noncharged anthracycline molecule; and Q_{10}, temperature coefficient.

Received 22 January 1998; accepted 18 May 1998.

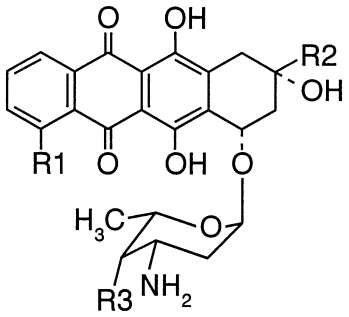

Compound	R1	R2	R3
1	OCH_3	$COCH_2OH$	OH
2	OCH_3	$COCH_3$	OH
3	H	$COCH_3$	OH
4	OCH_3	$COCH_2OH$	I
5	OCH_3	$CH(OH)CH_2OH$	I

FIG. 1. Chemical structure of the anthracycline derivatives studied: 1) doxorubicin; 2) daunorubicin; 3) 4-demethoxy-daunorubicin; 4) 4′-deoxy-4′-iododoxorubicin; and 5) 13-dihydro-4′-deoxy-4′-iododoxorubicin.

MATERIALS AND METHODS

Chemicals

Hydrochlorides of anthracyclines **1–5** were from Farmitalia. Stock solutions (1–2 mM) were prepared in distilled water or methanol and stored at −20°. Fatty acid-free BSA was obtained from Boehringer. Nigericin, BCECF-AM, and FITC-dextran (Mw 70,000) were from Sigma and Sephadex G-200 (fine) from Farmacia. All other chemicals and organic solvents were of analytical grade.

Buffer and Solvent Systems

The following buffer systems were used: (buffer 1), 57 mM of NaCl, 5.0 mM of KCl, 1.3 mM of $MgSO_4$, 9.0 mM of NaH_2PO_4, 51 mM of Na_2HPO_4 (pH 7.45); (buffer 2), 148.7 mM of NaCl, 22 mM of K_2HPO_4, 0.8 mM of KH_2PO_4, 1.2 mM of $MgSO_4$ (pH 7.45); and (buffer 3), 132 mM of KCl, 3.5 mM of NaCl, 10 mM of HEPES (pH 7.45). Millipore-filtered deionized water was used throughout. Lipids and anthracyclines were analyzed by TLC on 0.25 mm silica gel 60 plates (Merck) with the solvent systems: (A), $CHCl_3$-methanol-H_2O (32:12:2, v/v); (B), hexane-diethylether-acetic acid (35:15:0.5, v/v). Lipid compounds were visualized in iodine vapour and by a $CuSO_4$-H_3PO_4 char reagent.

Tumor Cells

The Ehrlich ascites tumor cell line EHR2/DNR+ [3] displaying the MDR phenotype was investigated. Resistance to **2** was developed and maintained *in vivo* by treating tumor-bearing mice with 1.6 mg **2**/kg, four times intraperitoneally per week [17, 18]. Tumor cells in the ascites fluid were removed and washed twice with buffer 1 by centrifugation at 800 *g* for 100 sec. The fraction of damaged cells was estimated to be 2–5% by trypan blue dye exclusion.

Cellular Uptake of Anthracycline

EHR2/DNR+ cells at a concentration of (1.00 ± 0.05) × 10^6/mL were incubated in the presence of the anthracycline compounds **1–5** (5.0 μM) in buffer 1 containing increasing concentrations of BSA (0–75 mg/mL). The buffer pH was readjusted to 7.45 ± 0.05. Experiments were performed at 27° and 37° in the presence of glucose (10 mM) or with cells pretreated with NaN_3 (10 mM) for 10 min before addition of anthracycline. The cellular drug content was measured as a function of time by extraction of cell pellets with a 0.3 M HCl-50% (v/v) ethanol solution at 25° as previously described [20, 21]. Concentrations of anthracycline were determined by means of spectrofluorometry using 1.00 μM standards of each of the anthracycline compounds (excitation wavelength 480 nm, emission wavelength 590 nm). Calibration curves were linear in the drug concentration range investigated and the recoveries of drug (free plus cell-associated) were ~95%.

Determination of Nuclear Anthracycline Binding

Measurements of the extent of nuclear binding of anthracyclines **1–4** were made by using cell suspensions in buffer 3 with a high K^+ concentration resembling the intracellular conditions and with addition of Triton X-100 to a final concentration of 0.1% (w/v) [22]. The dependence of binding on total drug concentrations ranging from 0.5 μM to 10 μM was measured in 30-min incubations at 37°. Control experiments confirmed that equilibrium was attained within less than 5 min. The nuclei were spun down at 3000 *g* for 100 sec and the amount of bound drug was determined as described above for intact cells. The concentration of nuclear binding sites in the cell cytoplasm and the apparent equilibrium binding constants (K_{DNA}) were estimated by analyzing plots of bound versus free drug concentrations by least-squares fitting. In the anthracycline concentration range investigated, satisfactory fits were provided using a simple binding model with identical and independent binding sites in the DNA. Calculations were carried out for a cell volume of 1000 μm^3. The binding parameters derived are included in the Appendix.

Determination of Anthracycline Binding to BSA

Equilibrium binding of anthracycline to BSA was determined using a Sephadex gel filtration method [16]. The experiments were performed with a 0.9 × 28 cm Sephadex G-200 gel column equilibrated and eluted at 22° with buffer 1 containing anthracyclines **1–5** (4–10 μM). Overall anthracycline binding constants (K_{BSA}) were calculated on the assumption of one binding site per albumin molecule [13, 23].

TABLE 1. Parameters for membrane diffusion of anthracyclines in EHR2/DNR+ cells

	J_{12}* (fmol/min/cell)	P_{plas}† (μm/min)	Q_{10}‡	pK_a§	P_{ow}¶	K_{lipid}** (mM^{-1})
1	0.062 ± 0.026	48	1.77	8.1–8.3	2.1	0.62
2	0.192 ± 0.059	147	2.43	8.0–8.2	8.9	1.89
3	1.290 ± 0.212	989	3.26	8.2–8.3	17.8	6.30
4	7.7	971		6.4	477	3.08
5	0.625 ± 0.041	79	2.95	6.4	174	2.11

* The rate measurements were performed at 37° in the presence of 10 mM of NaN_3 as in Fig. 2, with samples taken at intervals of 5–20 sec (**2**–**5**) or 5 min (**1**). Unidirectional influxes were derived from the slopes of regression fits to the initial linear phase of uptake. Values are means ± SD (N = 3–4). J_{12} for **4** was estimated on the basis of J_{12} = 2.628 ± 0.222 fmol/min/cell measured at 27° and Q_{10} = 2.95 measured for its 13-OH derivative (**5**).

† Apparent permeability coefficient of the plasma membrane to the noncharged drug molecule as calculated from the mean value of J_{12} using Eq. (1), a cell surface area equal to 1728 μm^2 [36] and pK_a = 8.2 (**1**–**3**) and 6.4 (**4**, **5**).

‡ Temperature coefficient as determined from rate measurements performed at 37° and 27°.

§ Acid dissociation constant. Data from [8, 12, 21, 29].

¶ 1-octanol/buffer (pH 7.45) partition coefficient. Data from [16].

** Overall binding affinity to liposomal phospholipid. Data from [16].

Determination of Intracellular pH

The cytosolic pH in EHR2/DNR+ cells was estimated with the fluorescent pH-probe BCECF-AM using pH-standard curves obtained with K^+/nigericin as described previously [24]. Measurements were performed at 37° with the BCECF-loaded cells (1×10^6 cells/mL) in buffer 1 with 10 mM of glucose or 10 mM of NaN_3. Intralysosomal pH was estimated by the FITC-dextran method [25]. Cell suspensions in RPMI 1640 culture medium (1×10^6 cells/mL) were incubated overnight at 37° with FITC-dextran at 1 mg/mL. The fluorescence measurements were performed at 37° in buffer 1 with 10 mM of glucose or 10 mM of NaN_3 (1×10^6 cells/mL). Results are included in the Appendix.

Determination of Total Cell Phospholipid

EHR2/DNR+ cells were extracted by $CHCl_3$-methanol [26] and the total phospholipid fraction was isolated on a silica gel column (2 × 10 cm, 230–400 mesh) washed with $CHCl_3$ (100 mL) and eluted with methanol (50 mL). The yield of phospholipid was 7.80 mg (41.5 μg/10^6 cells).

RESULTS

Determination of Initial Rates of Anthracycline Uptake

In an effort to examine the influence of serum albumin on the diffusional transbilayer movement of anthracyclines, a series of detailed kinetic experiments were performed with the Ehrlich ascites tumor cell line EHR2/DNR+. In a first set of experiments, initial rates of uptake for compounds **1**–**5** (Fig. 1) were measured with cell suspensions at 37° in a 60 mM phosphate buffer (buffer 1, pH 7.45) containing 10 mM of NaN_3 to exclude any interference from energy-dependent transport mechanisms. It is most important that EHR2/DNR+ cells remain intact under these particular conditions [27]. Following rapid mixing of the cells with anthracycline (5.0 μM), serial samples were removed at time intervals for analysis of the total cellular drug content by extraction into acid methanol/water. For all but the most lipophilic compound **4**, the time-courses of drug uptake were composed of a very rapid (<5 sec) initial phase followed by a linear phase over a period of 1–10 min consistent with previous studies [18, 28]. J_{12}s were calculated from regression fits to the linear phase. Results are given in Table 1. In the case of **4**, the initial uptake kinetics was too rapid to be measured. All the experiments were therefore repeated at 27° where influx rates are reduced [28]. J_{12} for **5**, the 13-OH derivative of **4**, was reduced from 0.625 ± 0.041 to 0.212 ± 0.003 fmol/min/cell (means ± SD, N = 4) corresponding to a Q_{10} = 2.95. Using this value and a measured J_{12} = 2.628 ± 0.222 fmol/min/cell (N = 4) of **4** at 27°, the predicted influx rate of **4** at 37° would be about 7.7 fmol/min/cell. As found previously [28], the Q_{10} values varied significantly even between the closely related derivatives (see Table 1). For this reason, the above J_{12} value of **4** at 37° can only be taken as an estimate.

The apparent P_{plas} of the cell membrane to compounds **1**–**5** in their noncharged form was estimated from the calculated J_{12} values using the relation:

$$J_{12} = P_{plas}\, S_{plas}\, \beta\, [A]_1 \qquad (1)$$

where S_{plas} is the cell surface area, β the fractional anthracycline ionization, and $[A]_1$ the concentration of anthracycline monomer in the extracellular aqueous phase. β is calculated by the following equation:

$$\beta = 1/(1 + 10^{pKa-pH1}) \qquad (2)$$

where pK_a is the acid dissociation constant for the drug as determined by pH-titration in aqueous medium [8, 12, 21, 29] and pH_1 the extracellular medium pH. On the basis of previous studies [30–35], it was assumed that only the noncharged molecules cross the cell membrane. A cell surface area equal to 1728 μm^2, obtained in a morphometric analysis [36], was used in the calculations. Results are included in Table 1. Also listed in Table 1 are data on anthracycline lipophilicity as measured by the P_{ow} and the overall K_{lipid} to phospholipid in small unilamellar vesicles

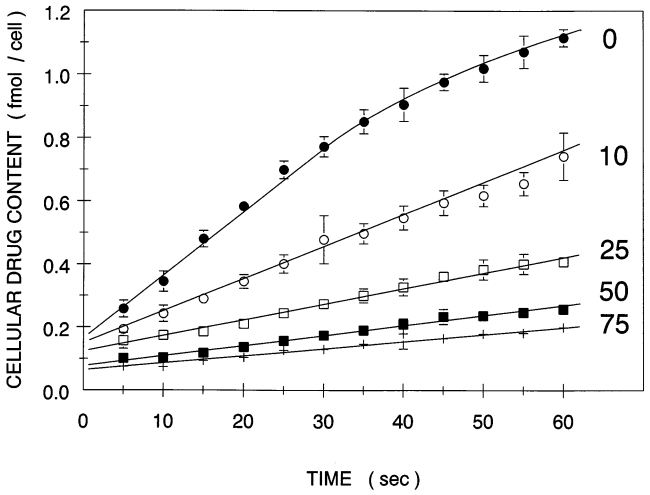

FIG. 2. Effect of BSA on the initial uptake of 4-demethoxydaunorubicin (3) in EHR2/DNR+ cells. Cell suspensions (1×10^6 cells/mL) were preincubated for 10 min at 37° in buffer 1 containing 10 mM of NaN_3 and varying BSA concentrations: 0 (●), 10 (○), 25 (□), 50 (■), and 75 mg/mL (+) as indicated. 3 was added at zero time with rapid mixing from a stock solution in water (2 mM) to a final concentration of 5.0 μM. Serial samples were withdrawn at 5-sec time intervals and the total cellular drug content was determined using a fluorescence-based method as described in Materials and Methods. Data points are means ± SD from three independent sets of experiments.

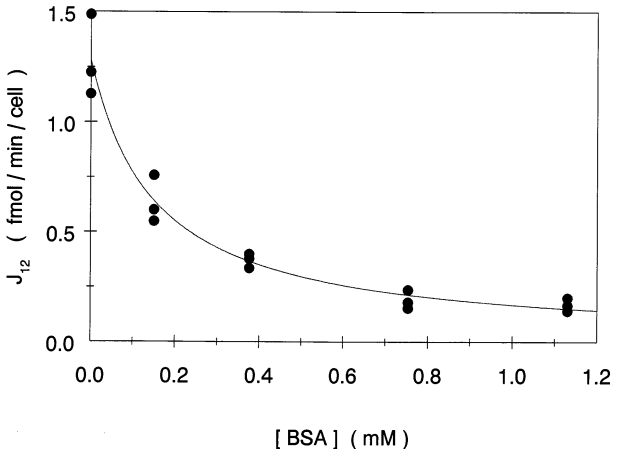

FIG. 3. Dependence of J_{12} on BSA concentration. Rate measurements with EHR2/DNR+ cells (buffer 1, 10 mM of NaN_3, 37°) were done with 4-demethoxydaunorubicin (3, 5.0 μM) in the presence of varying concentrations of BSA (0–75 mg/mL, 0–1.13 mM) as in Fig. 2 with samples taken at intervals of 5 sec. Data points are from three independent sets of experiments. The fitting-curve is drawn using Eq. (3) with the following values: $K_{BSA} = 6.64\ mM^{-1}$, $(J_{12})_0 = 1.29$ fmol/min/cell.

prepared from the EHR2/DNR+ cell phospholipid fraction [16]. Our finding that J_{12} and P_{plas} increase with the lipophilicity of the anthracycline molecule is consistent with a number of studies [9, 10, 15, 18, 32, 37]. In the calculation of P_{plas} according to Eq. (1), a linear relationship between J_{12} and the aqueous phase concentration of free anthracycline is assumed. This has been experimentally confirmed in EHR2 cells for **2** up to 5 μM in previous studies [28, 38]. However, in the case of the more lipophilic compounds, this linearity may not hold due to the formation of drug dimers with a reduced membrane permeability [30]. By using the dimerization constant of **3** ($4.3\ mM^{-1}$) and **4** ($21.1\ mM^{-1}$) reported in [13], approximately 4 and 15%, respectively, is estimated to be present as dimers at 5 μM. The values for P_{plas} listed in Table 1 were not corrected for this extent of dimerization.

Effect of Serum Albumin on the Initial Rates of Anthracycline Uptake

A gradual reduction in the J_{12} values for **1**, **2**, **3**, and **4** (5.0 μM) was measured when BSA was added from 0 to 75 mg/mL (0–1.13 mM) to the cell suspensions containing 10 mM of NaN_3. The data for **3** are given in Fig. 2, which shows the initial drug uptake measured over a 60-sec period. A plot of J_{12} versus albumin concentration ([BSA]) is shown in Fig. 3. The line through the data points represents a least-squares fit to the equation:

$$(J_{12})_{BSA} = (J_{12})_0/(1 + K_{BSA}\,[BSA]) \qquad (3)$$

where $(J_{12})_{BSA}$ and $(J_{12})_0$ are the influx rates in the presence and absence of BSA, respectively, and K_{BSA} the overall anthracycline–albumin binding constant. This simple relation is obtained by assuming that $(J_{12})_{BSA}$ is directly proportional to the aqueous phase concentration of free anthracycline in rapid equilibrium with the BSA. It appears that the relation satisfactorily explains the effect which BSA has on the influx rate of **3**. Similar results were obtained with compounds **1**, **2**, and **4** (data not shown). The calculated K_{BSA} values are listed in Table 2.

Effect of Serum Albumin on Anthracycline Uptake Kinetics in Medium with NaN_3

The effect of medium BSA on the kinetics of uptake of compounds **1**–**4** was determined over a 120-min incubation

TABLE 2. Overall binding constants (K_{BSA}) of anthracycline derivatives for BSA

	K_{BSA} (mM^{-1})*		
	From $(J_{12})_{BSA}$†	From A_{st}‡	From gel filtration§
1	1.06 ± 0.40		1.54 ± 0.24
2	1.11 ± 0.14	1.17 ± 0.23	2.87 ± 0.12
3	6.64 ± 1.98	11.0 ± 0.7	18.0 ± 1.3
4	34.6 ± 0.9	27.6 ± 2.2	51.6 ± 4.0

* All values are means ± SD (N = 3–4).

† Calculated from plots of $(J_{12})_{BSA}$ versus BSA concentration (0–1.13 mM) as described in Fig. 3 and using Eq. (3). For **4**, the calculations were based on rate measurements in the presence of 0.15–1.13 mM of BSA and an estimated value of $(J_{12})_0$ = 7.7 fmol/min/cell (see Table 1).

‡ Calculated by fitting theoretical accumulation curves to the steady state (A_{st}) reached at various BSA concentrations (0–75 mg/mL, 0–1.13 mM) as in Figs. 4 and 5. Steady state for **1** was not reached within the 120-min incubation period.

§ Equilibrium binding constants determined from Sephadex G-200 gel filtration.

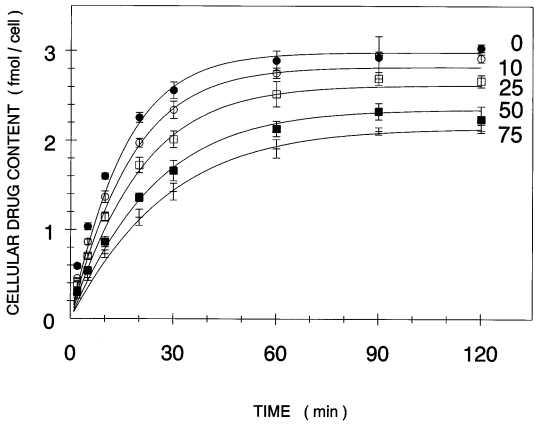

FIG. 4. Effect of BSA on the time-course of daunorubicin (2, 5.0 μM) uptake in EHR2/DNR+ cells. Drug uptake (buffer 1, 10 mM of NaN_3, 37°) was measured in the presence of varying BSA concentrations (0–75 mg/mL). Symbols as in Fig. 2. The values (means ± SD) from three independent experiments are corrected for the contribution of the "absorptive" drug uptake (0.06–0.3 fmol/cell). The lines through the data points are the theoretical accumulation curves calculated for each BSA concentration using K_{BSA} = 1.17 mM^{-1} and P_{plas} = 147 μm/min. The mathematical model for computer simulation of the uptake kinetics and model parameters are given in the Appendix.

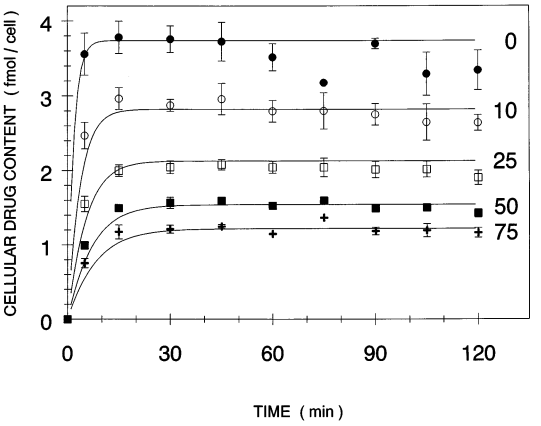

FIG. 5. Effect of BSA on the time-course of 4-demethoxydaunorubicin (3, 5.0 μM) uptake obtained for EHR2/DNR+ cells in a medium containing NaN_3 (buffer 1, 10 mM of NaN_3, 37°). Experimental conditions, BSA concentrations (0–75 mg/mL) and symbols as in Fig. 4. Data points (means ± SD) are from three independent experiments. Theoretical accumulation curves (lines) are calculated using the model parameters: K_{BSA} = 11.0 mM^{-1} and P_{plas} = 989 μm/min. The component of "absorptive" drug uptake was 0.06–0.30 fmol/cell.

in the presence of NaN_3. During this period, a steady-state (A_{st}) was reached except for **1** with a slow rate of uptake. As can be seen from Fig. 4, which gives a data set for **2**, addition of increasing concentrations of albumin (0–75 mg/mL) was found to cause a gradual reduction in A_{st} as well as in J_{12}. The data in Fig. 4 were analyzed by means of numerical computer simulations according to the kinetic model given in the Appendix section. Theoretical time-courses for drug accumulation were computed using P_{plas} = 147 μm/min determined from the initial rate measurements (Table 1), and Eq. (3) was used to express the relation between [BSA] and the drug influx rate. In addition, the calculations were based on measurements of the intracellular pH, total cell phospholipid, and nuclear anthracycline binding parameters as described in Materials and Methods. The results of these measurements are listed in the Appendix together with other parameters taken from the model previously developed in our laboratory [19]. Using K_{BSA} = 1.17 mM^{-1}, it was possible to fit the theoretical time-course for uptake of **2** to the experimental data in the [BSA] range investigated. This is shown by the lines through the data points in Fig. 4. The magnitude of the reduction in A_{st} obtained in the presence of medium BSA was larger for **3** (Fig. 5) and **4** (data not shown) than for **2**, in agreement with an increased affinity for BSA. The K_{BSA} values determined by computer simulation of the time-courses for each compound are given in Table 2. All calculations were performed after a correction of the experimental data for the contribution of "absorptive" drug uptake due to rapid drug binding to damaged cells. This component (0.10–0.36 fmol/cell) was estimated from the y-axis intercept of the fitting-line to the initial linear phase of each uptake curve (see Fig. 2).

Effect of Serum Albumin on Anthracycline Uptake Kinetics in Medium with Glucose

In the final experiments, we examined the kinetics of uptake of compounds **2–4** in a medium with 10 mM of glucose. Consistent with our previous results [17, 18], the difference between the A_{st} value reached for each compound in the presence of glucose and the corresponding value in the presence of NaN_3 narrows as drug membrane permeability increases. The data are reported in Table 3. The theoretical rate of glucose-dependent drug efflux required to obtain the measured reduction in A_{st} was then estimated using our kinetic model where Pgp is the main glucose-dependent efflux mechanism ($J_{21,P}$, see Fig. 7 in the Appendix). In addition, with reference to the results in [28, 38], we assume that the diffusional transbilayer movement

TABLE 3. Steady-state levels of anthracycline uptake (A_{st}) and calculated steady-state rates of energy-dependent anthracycline efflux ($J_{21,P}$) in EHR2/DNR+ cells

	A_{st} (fmol/cell)*		$J_{21,P}$ (fmol/min/cell)†
	+ NaN_3	+ glucose	
2	3.00 ± 0.20	0.51 ± 0.19	0.138–0.162
3	3.49 ± 0.29	3.06 ± 0.26	0.139–0.309
4	3.24 ± 0.46	3.12 ± 0.51	0–1.8

* Time-courses of anthracycline uptake were determined over a 120-min period (buffer 1, 37°, 5.0 μM anthracycline) in the presence of either NaN_3 (10 mM) or glucose (10 mM). A_{st} values were calculated with a correction for the "absorptive" component of drug uptake (0.15–0.36 fmol/cell). Values are means ± SD from 3–5 determinations in two separate sets of experiments.

† Theoretical values of $J_{21,P}$ were determined by analyzing time-courses for each of the compounds using the kinetic model in the Appendix. Calculations were done for the P_{plas} values determined in medium with NaN_3 (147 (**2**), 989 (**3**), and 971 (**4**) μm/min), and $J_{21,P}$ was adjusted to fit the calculated A_{st} to the experimental data. Other model parameters are defined in the Appendix. Values are the data range from analysis of 3–5 time-courses.

of anthracycline in a medium with glucose is similar to that in a medium with NaN_3. In the data fitting, $J_{21,P}$ was adjusted until the A_{st} value reached for the simulated drug accumulation curve showed the best agreement with the experimental data. As can be seen from Table 3, the uptake data could be fitted using a range of $J_{21,P}$ values within the experimental error. Compound **3** was chosen in subsequent experiments to determine the effect of serum albumin on the drug uptake kinetics. Time-courses for uptake of **3** were determined in a medium with varying [BSA] (0–75 mg/mL) under conditions as in Fig. 5 except for the presence of glucose instead of NaN_3. A data set is shown in Fig. 6. Theoretical accumulation curves were computed for each BSA concentration using K_{BSA} = 11.0 mM^{-1} and P_{plas} = 989 μm/min (data from Fig. 5), and the model parameter $J_{21,P}$ was altered to fit the experimental data. The apparent Michaelis constant for the glucose-dependent efflux mechanism was set at K_m = 1 μM in accord with the values (0.5–3 μM) measured for Pgp transport of anthracyclines [39–42]. As the calculated lines through the data points in Fig. 6 demonstrate, a reasonably good fit to the data was obtained over the whole [BSA] range using $J_{21,P}$ = 0.20 fmol/min/cell. Assuming 10^6 molecules of Pgp per cell, as determined by freeze-fracture electron microscopy of EHR2/DNR+ cells [43], this value corresponds to 0.71 μmol of anthracycline transported/min/mg Pgp. Interestingly, this figure falls within the range of reported ATPase activities for purified and reconstituted Pgp [44, 45]. We conclude that the theoretical analysis provides parameters that allow us to predict the anthracycline uptake kinetics in a relevant cell medium with glucose and serum albumin.

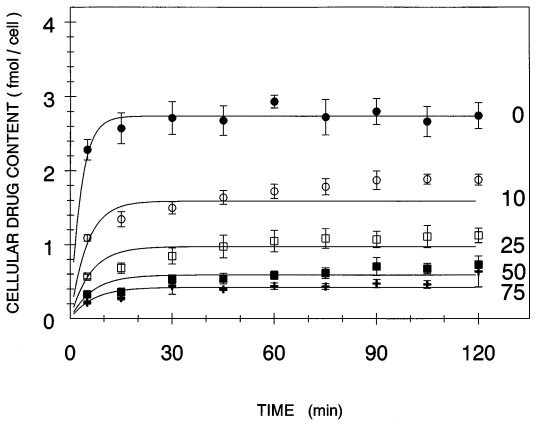

FIG. 6. Effect of BSA on the time-course of 4-demethoxydaunorubicin (3, 5.0 μM) uptake obtained for EHR2/DNR+ cells in a medium containing glucose. Experimental conditions as in Fig. 5 except for the presence of 10 mM of glucose instead of NaN_3. Data points (means ± SD) are from three independent experiments. The theoretical accumulation curves (lines) are calculated using the model parameters: K_{BSA} = 11.0 mM^{-1}, P_{plas} = 989 μm/min, $J_{21,P}$ = 0.20 fmol/min/cell and K_m = 1 μM. The component of "absorptive" uptake was 0.03–0.10 fmol/cell.

DISCUSSION

Although plasma protein binding of anthracyclines is well documented [46], only a few basic studies have implicated this binding in a kinetic analysis of cellular drug uptake. In early studies [47], Dalmark and Johansen demonstrated that plasma proteins strongly affect the rate at which **1** enters red blood cells. Broxterman *et al.* [48] analyzed the effect of BSA on the uptake of **2** into an ovarian carcinoma cell line. However, no significant effect was observed in the presence of either 10 or 40 mg of BSA per mL. In a recent study with rat hepatocytes by Rivory *et al.* [15], the uptake of **1** and **4** over a 30-min period was reduced by a factor of 2.3 and 7.9, respectively, in the presence of BSA (40 mg/mL). The corresponding factors in our experiments were 1.3 and 2.4 (data not shown). Most importantly, our data on the uptake kinetics of **2** and **3** (Figs. 4 and 5) demonstrate, in agreement with [15], that a lipophilic anthracycline derivative with high membrane permeability and an increased cellular uptake in a test medium without serum albumin may in fact show a decreased uptake when compared to the parent (less lipophilic) compound in a system with physiologically relevant serum albumin concentrations (40–50 mg/mL).

When attempting to predict the pharmacokinetics of new anthracycline compounds in a structure-based drug design, it is essential to establish a quantitative relation between the parameters K_{BSA}, P_{plas}, and drug molecular structure. The complexity of this relation is evident from a number of recent studies. First, in serum albumin there are indications of a flexible anthracycline binding domain close to positively charged amino acid residues [13, 23, 49]. Polar as well as hydrophobic interactions contribute to the anthracycline–albumin complex formation and, as shown in Table 2, K_{BSA} values vary over a wide range. Second, according to the solubility-diffusion model for simple diffusion of small lipophilic molecules across lipid bilayers [5, 50], P_{plas} can be assumed to be proportional to the product of two parameters: 1) the membrane/water partition coefficient of the diffusing anthracycline molecule as measured by K_{lipid}, and 2) the overall diffusion coefficient (D_{lipid}) of the drug molecule within the membrane lipid phase. K_{lipid} has been measured for a number of anthracyclines in liposomal model membranes [16, 51, 52]. Unfortunately, few experimental data are available on the relation between drug structure and D_{lipid}. From the values of K_{lipid} known for compounds **1–5** from our study [16], it is possible to comment on this relation with reference to the permeability data in Table 1. For compounds **1–3** and **5**, the increase in P_{plas} is found to parallel the increase in K_{lipid} within the uncertainty of the experimental data. Thus, for these compounds, a change in the hydrogen-bonding capability and overall hydrophobicity does not appear to greatly influence the D_{lipid} value. In the case of **4**, the measured P_{plas} was much higher than expected from the value of K_{lipid}. This discrepancy may be due in part to the uncertainty in the determination of J_{12} or to a more complex association–dissociation reaction of this lipophilic compound with membrane lipid.

Current models for the transfer of hydrophobic ligands such as bilirubin [53] and long-chain fatty acids [54] between serum albumin and lipid membranes are based on a mechanism with dissociation of the ligand–albumin complex in a first step, followed by diffusion of the free ligand onto the cell surface via the aqueous phase in a second step. The fact that our data on the relation between J_{12} and [BSA] fit well with Eq. (3) over a wide range of K_{BSA} values provides strong evidence that a similar two-step diffusional process applies to the cellular uptake of albumin-bound anthracycline. Also, our estimates of K_{BSA} obtained from the rate measurements agree quite well in all cases (within a factor of about 2) with the values determined directly by Sephadex G-200 gel filtration (Table 2). Thus, we conclude from these data that the effect of BSA on diffusional anthracycline uptake is a direct consequence of an altered distribution between free and protein-bound drug molecules in the bulk aqueous phase. We can rule out the possibility that the cell membrane changes its anthracycline permeability upon interaction with serum albumin. This is a most important conclusion, because predictions can then be made on the uptake kinetics of new anthracycline compounds under physiologically relevant serum conditions. It also makes it possible to analyze drug uptake kinetics in the case of water-insoluble anthracycline derivatives where inclusion of medium serum albumin is needed to prevent drug precipitation.

Although simplified, our mathematical simulation model seems adequate for the purpose of analyzing the effect of serum albumin on anthracycline accumulation in MDR tumor cells. This suggests interesting possibilities for making predictions on the extent to which protein binding may influence the clinical applicability of new anthracycline compounds by using appropriate biomathematical simulation methods. The next central question within the framework of our kinetic model therefore concerns the correlation between drug transport parameters and drug interactions with the nuclear enzyme topoisomerase II responsible for anthracycline cytotoxicity [55]. In our previous work [18], the cytotoxicity of compounds **1** and **4** in EHR2/DNR2 cells was compared in a clonogenic assay. However, attempts to examine the formation of topoisomerase–DNA complexes in this cell line failed in experiments with anthracyclines, and the specific topoisomerase II inhibitor VM-26 was used instead [56, 57]. A more precise analysis of anthracycline cytotoxicity versus transport will require further study.

This work was supported by grants from The Danish Cancer Society (94-018) (E.J.F.D), The Novo Nordisk Fund (E.J.F.D), The Danish Cancer Research Fund (E.F), and The Pharmacy Foundation of 1991 (E.F). We gratefully acknowledge the expert technical assistance of Mrs Inge Kobbernagel.

APPENDIX

Numerical Analysis of Anthracycline Accumulation Data

Theoretical time-courses for anthracycline accumulation in EHR2/DNR+ cells were computed on the basis of the 3-compartment transport model published previously [19], with the main modification being that extracellular anthracycline is in equilibrium with binding sites on serum albumin. To simplify the model, the contribution of vesicular drug transport is neglected (<0.2% of the total). Drug trapping in acidic vesicles is maintained (5–10% of the total). A schematic representation of the model cell is given in Fig. 7. Anthracycline interactions with the main nuclear target enzyme topoisomerase II are illustrated in the model. The model calculations assume reversibility of all binding reactions. Plots of total cell-associated anthracycline versus time with 100–200 data points were produced by numerical integration of the rate equations. A set of model parameters was built up from the literature and on the basis of experiments in the present study. The following definitions and values have been used with reference to [19]:

1. Acid dissociation constant for anthracycline (pK_a): 8.2 (**1**, **2**, **3**) [8, 21, 29]; 6.4 (**4**, **5**) [12].
2. pH in extracellular medium (pH_1): 7.45.
3. pH in cell cytoplasm (pH_2): 7.61 (medium with glucose); 7.32 (medium with NaN_3) (present study).
4. pH in endosomal vesicles (pH_3): 5.0 (medium with glucose); 6.0 (medium with NaN_3) (present study).
5. Total concentration of extracellular anthracycline at zero time ($[A]_1$): 5.0 μM.
6. Apparent permeability coefficient of the plasma membrane to the noncharged anthracycline molecule (P_{plas}): range 30–1000 μm/min.
7. Apparent permeability coefficient of the endosomal membranes to the noncharged anthracycline molecule (P_{endo}): range 30–1000 μm/min.

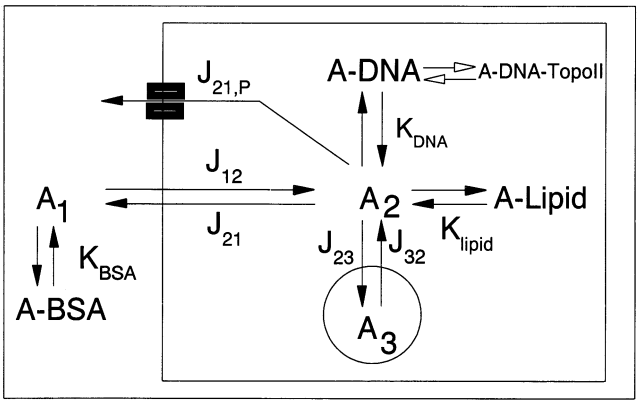

FIG. 7. Model cell for computer simulation of anthracycline accumulation. Symbols and model parameters are defined in the Appendix. Also indicated in the model is anthracycline interaction with the nuclear target enzyme topoisomerase II forming a ternary anthracycline–DNA–topoisomerase II complex (A-DNA-TopoII).

8. Extracellular medium volume per cell at 10^6 cells per mL (V_1): 10^6 μm^3.
9. Volume of cell cytoplasm (V_2): 1000 μm^3. A mean total cell volume of 1071 μm^3 is estimated by electron microscopy and morphometric analysis [36].
10. Volume of acidic vesicles (V_3): 25 μm^3 [36].
11. Surface area of plasma membrane (S_{plas}): 1728 μm^2 [36].
12. Surface area of acidic vesicles (S_{endo}): 333 μm^2 [36].
13. Concentration of extracellular BSA ([BSA]): range 0–75 mg/mL (0–1.13 mM).
14. Overall anthracycline binding constant for BSA (K_{BSA}): range 1–52 mM^{-1} (present study).
15. Concentration of membrane lipid in V_2 ($[L_1]$): 55 mM. Calculated on basis of 41.5 μg lipid per 10^6 cells and V_2 = 1000 μm^3 (present study).
16. Overall anthracycline binding constant for membrane lipid (K_{lipid}): range 0.62–6.30 mM^{-1} [16].
17. Concentration of nuclear binding sites for anthracycline ($[D_T]$): range 4.80–5.80 mM. Calculated on basis of V_2 = 1000 μm^3 (present study).
18. Apparent DNA binding constant for anthracycline (K_{DNA}): 1.00 × 10^6 M^{-1} (**1**), 0.41 × 10^6 M^{-1} (**2**), 0.60 × 10^6 M^{-1} (**3**), 0.54 × 10^6 M^{-1} (**4**) (present study).
19. Dimerization constant for anthracycline (K_3): 13 mM^{-1} (**1**), 23 mM^{-1} (**2**) [58]; 4.3 (**3**), 21.1 (**4**) [13].
20. Apparent Michaelis constant for anthracycline transporter (K_m): 1 μM.
21. Number of anthracycline transporter molecules per cell (N_p): 10^6 [43].
22. Catalytic constant for anthracycline transporter (C_p): range 0–1000 min^{-1}.

References

1. Gottesman MM and Pastan I, Biochemistry of multidrug resistance mediated by the multidrug transporter. *Annu Rev Biochem* **62:** 385–427, 1993.
2. Rosenberg MF, Callaghan R, Ford RC and Higgins CF, Structure of the multidrug resistance P-glycoprotein to 2.5 nm resolution determined by electron microscopy and image analysis. *J Biol Chem* **272:** 10685–10694, 1997.
3. Danø K, Active outward transport of daunomycin in resistant Ehrlich ascites tumor cells. *Biochim Biophys Acta* **323:** 466–483, 1973.
4. Skovsgaard T, Mechanisms of resistance to daunorubicin in Ehrlich ascites tumor cells. *Cancer Res* **38:** 1785–1791, 1978.
5. Stein WD, Kinetics of the multidrug transporter (P-glycoprotein) and its reversal. *Physiol Rev* **77:** 545–590, 1997.
6. Danø K, Development of resistance to adriamycin (NSC-123127) in Ehrlich ascites tumor *in vivo*. *Cancer Chemother Rep* **56:** 321–326, 1972.
7. Coley HM, Twentyman PR and Workman P, Improved cellular accumulation is characteristic of anthracyclines which retain high activity in multidrug-resistant cell lines, alone or in combination with verapamil or cyclosporin A. *Biochem Pharmacol* **24:** 4467–4475, 1989.
8. Facchetti I, Grandi M, Cucchi P, Geroni C, Penco S and Vigevani A, Influence of lipophilicity on cytotoxicity of anthracyclines in LoVo and LoVo/Dx human cell lines. *Anti-Cancer Drug Design* **6:** 385–397, 1991.
9. Mülder HS, Dekker H, Pinedo HM and Lankelma J, The P-glycoprotein-mediated relative decrease in cytosolic free drug concentration is similar for several anthracyclines with varying lipophilicity. *Biochem Pharmacol* **50:** 967–974, 1995.
10. Lampidis TJ, Kolonias D, Podona T, Israel M, Safa AR, Lothstein L, Savaraj N, Tapiero H and Priebe W, Circumvention of P-GP MDR as a function of anthracycline lipophilicity and charge. *Biochemistry* **36:** 2679–2685, 1997.
11. Supino R, Necco A, Dasdia T, Casazza AM and Di Marco A, Relationship between effects on nucleic acid synthesis in cell cultures and cytotoxicity of 4-demethoxy derivatives of daunorubicin and adriamycin. *Cancer Res* **37:** 4523–4528, 1977.
12. Barbieri B, Giuliani FC, Bordoni T, Casazza AM, Geroni C, Bellini O, Suarato A, Gioia B, Penco S and Arcamone F, Chemical and biological characterization of 4′-iodo-4′-deoxydoxorubicin. *Cancer Res* **47:** 4001–4006, 1987.
13. Rivory LP, Pond SM and Winzor DJ, The influence of pH on the interaction of lipophilic anthracyclines with bovine serum albumin. Quantitative characterization by measurements of fluorescence quenching. *Biochem Pharmacol* **44:** 2347–2355, 1992.
14. Chassany O, Urien S, Claudepierre P, Bastian G and Tillement JP, Comparative serum protein binding of anthracycline derivatives. *Cancer Chemother Pharmacol* **38:** 571–573, 1996.
15. Rivory LP, Avent KM and Pond SM, Effects of lipophilicity and protein binding on the hepatocellular uptake and hepatic disposition of two anthracyclines, doxorubicin and iododoxorubicin. *Cancer Chemother Pharmacol* **38:** 439–445, 1996.
16. Demant EJF and Friche E, Equilibrium binding of anthracycline cytostatics to serum albumin and small unilamellar phospholipid vesicles as measured by gel filtration. *Biochem Pharmacol* **55:** 27–32, 1998.
17. Friche E, Jensen PB, Roed H, Skovsgaard T and Nissen NI, *In vitro* circumvention of anthracycline-resistance in Ehrlich ascites tumour by anthracycline analogues. *Biochem Pharmacol* **39:** 1721–1726, 1990.
18. Friche E, Jensen PB, Skovsgaard T and Nissen NI, Evaluation of 4′-deoxy-4′-iododoxorubicin in sensitive and multidrug-resistant Ehrlich ascites tumour. *J Cell Pharmacol* **1:** 57–65, 1990.
19. Demant EJF, Sehested M and Jensen PB, A model for computer simulation of P-glycoprotein and transmembrane ΔpH-mediated anthracycline transport in multidrug-resistant tumor cells. *Biochim Biophys Acta* **1055:** 117–125, 1990.
20. Bachur NR, Moore AL, Bernstein IG and Liu A, Tissue distribution and disposition of daunomycin (NSC-82151) in mice: fluorometric and isotopic methods. *Cancer Chemother Rep* **54:** 89–94, 1970.
21. Skovsgaard T, Transport and binding of daunorubicin, adriamycin, and rubidazone in Ehrlich ascites tumor cells. *Biochem Pharmacol* **26:** 215–222, 1977.
22. Tarasiuk J, Frezard F, Garnier-Suillerot A and Gattegno L, Anthracycline incorporation in human lymphocytes. Kinetics of uptake and nuclear concentrations. *Biochim Biophys Acta* **1013:** 109–117, 1989.
23. Demant EJF and Sehested M, Recognition of anthracycline binding domains in bovine serum albumin and design of a free fatty acid sensor protein. *Biochim Biophys Acta* **1156:** 151–160, 1993.
24. Frezard F and Garnier-Suillerot A, Determination of the osmotic active drug concentration in the cytoplasm of anthracycline-resistant and -sensitive K562 cells. *Biochim Biophys Acta* **1091:** 29–35, 1991.
25. Ohkuma S, Use of fluorescein isothiocyanate-dextran to

measure proton pumping in lysosomes and related organelles. *Methods Enzymol* **174:** 131–154, 1989.
26. Folch J, Ascoli I, Lees M, Meath JA and LeBaron FN, Preparation of lipid extracts from brain tissue. *J Biol Chem* **191:** 833–841, 1951.
27. Rasmussen J, Hansen LL, Friche E and Jaroszewski JW, ^{31}P and ^{13}C NMR spectroscopic study of wild-type and multidrug-resistant Ehrlich ascites tumor cells. *Oncol Res* **5:** 119–126, 1993.
28. Skovsgaard T, Carrier-mediated transport of daunorubicin, adriamycin, and rubidazone in Ehrlich ascites tumour cells. *Biochem Pharmacol* **27:** 1221–1227, 1978.
29. Frezard F and Garnier-Suillerot A, Comparison of the binding of anthracycline derivatives to purified DNA and to cell nuclei. *Biochim Biophys Acta* **1036:** 121–127, 1990.
30. Dalmark M and Storm HH, A fickian diffusion transport process with features of transport catalysis. Doxorubicin transport in human red blood cells. *J Gen Physiol* **78:** 349–364, 1981.
31. Frezard F and Garnier-Suillerot A, DNA-containing liposomes as a model for the study of cell membrane permeation by anthracycline derivatives. *Biochemistry* **30:** 5038–5043, 1991.
32. Frezard F and Garnier-Suillerot A, Comparison of the membrane transport of anthracycline derivatives in drug-resistant and drug-sensitive K562 cells. *Eur J Biochem* **196:** 483–491, 1991.
33. Siegfried JM, Burke TG and Tritton TR, Cellular transport of anthracyclines by passive diffusion. Implications for drug resistance. *Biochem Pharmacol* **34:** 593–598, 1985.
34. Roepe PD, The role of the MDR protein in altered drug translocation across tumor cell membranes. *Biochim Biophys Acta* **1241:** 385–406, 1995.
35. Cullis PR, Hope MJ, Bally MB, Madden TD, Mayer LD and Fenske DB, Influence of pH gradients on the transbilayer transport of drugs, lipids, peptides and metal ions into large unilamellar vesicles. *Biochim Biophys Acta* **1331:** 187–211, 1997.
36. Sehested M, Skovsgaard T, Van Deurs B and Winther-Nielsen H, Increase in nonspecific adsorptive endocytosis in anthracycline- and vinca alkaloid-resistant Ehrlich ascites tumor cell lines. *J Natl Cancer Inst* **78:** 171–179, 1987.
37. Frézard F and Garnier-Suillerot A, Permeability of lipid bilayer to anthracycline derivatives. Role of the bilayer composition and of the temperature. *Biochim Biophys Acta* **1389:** 13–22, 1998.
38. Nielsen D, Maare C and Skovsgaard T, Influx of daunorubicin in multidrug-resistant Ehrlich ascites tumour cells: Correlation to expression of P-glycoprotein and efflux. Influence of verapamil. *Biochem Pharmacol* **50:** 443–450, 1995.
39. Spoelstra EC, Westerhoff HV, Dekker H and Lankelma J, Kinetics of daunorubicin transport by P-glycoprotein of intact cancer cells. *Eur J Biochem* **207:** 567–579, 1992.
40. Pereira E, Borrel MN, Fiallo M and Garnier-Suillerot A, Non-competitive inhibition of P-glycoprotein-associated efflux of THP–adriamycin by verapamil in living K562 leukemia cells. *Biochim Biophys Acta* **1225:** 209–216, 1994.
41. Borrel MN, Fiallo M, Priebe W and Garnier-Suillerot A, P-glycoprotein-mediated efflux of hydroxyrubicin, a neutral anthracycline derivative, in resistant K562 cells. *FEBS Lett* **356:** 287–290, 1994.
42. Ghauharali RI, Westerhoff HV, Dekker H and Lankelma J, Saturable P-glycoprotein kinetics assayed by fluorescence studies of drug efflux from suspended human KB8–5 cells. *Biochim Biophys Acta* **1278:** 213–222, 1996.
43. Sehested M, Simpson D, Skovsgaard T and Jensen PB, Freeze-fracture study of plasma membranes of wild-type and daunorubicin-resistant Ehrlich ascites tumor and P388 leukemia cells. *Virchows Arch B Cell Pathol* **56:** 327–335, 1989.
44. Sharom FJ, Yu X and Doige CA, Functional reconstitution of drug transport and ATPase activity in proteoliposomes containing partially purified P-glycoprotein. *J Biol Chem* **268:** 24197–24202, 1993.
45. Urbatsch IL, Al-Shawi MK and Senior AE, Characterization of the ATPase activity of purified Chinese hamster P-glycoprotein. *Biochemistry* **33:** 7069–7076, 1994.
46. Eksborg S, Ehrsson H and Ekqvist B, Protein binding of anthraquinone glycosides, with special reference to adriamycin. *Cancer Chemother Pharmacol* **10:** 7–10, 1982.
47. Dalmark M and Johansen P, Molecular association between doxorubicin (adriamycin) and DNA-derived bases, nucleosides, nucleotides, other aromatic compounds, and proteins in aqueous solution. *Mol Pharmacol* **22:** 158–165, 1982.
48. Broxterman HJ, Kuiper CM, Schuurhuis GJ, Van der Hoeven JJM, Pinedo HM and Lankelma J, Daunomycin accumulation in resistant tumor cells as a screening model for resistance-modifying drugs: Role of protein binding. *Cancer Lett* **35:** 87–95, 1987.
49. Demant EJF, Jensen PB and Sehested M, Characterization of the cooperative cross-linking of doxorubicin N-hydroxysuccinimide ester derivatives to water-soluble proteins. *Biochim Biophys Acta* **1118:** 83–90, 1991.
50. Lieb WR and Stein WD, Non-stokesian nature of transverse diffusion within human red cell membranes. *J Membrane Biol* **92:** 111–119, 1986.
51. Burke TG and Tritton TR, Structural basis of anthracycline selectivity for unilamellar phosphatidylcholine vesicles: An equilibrium binding study. *Biochemistry* **24:** 1768–1776, 1985.
52. Gallois L, Fiallo M, Laigle A, Priebe W and Garnier-Suillerot A, The overall partitioning of anthracyclines into phosphatidyl-containing model membranes depends neither on the drug charge nor the presence of anionic phospholipids. *Eur J Biochem* **241:** 879–887, 1996.
53. Zucker SD, Goessling W and Gollan JL, Kinetics of bilirubin transfer between serum albumin and membrane vesicles. Insight into the mechanism of organic anion delivery to the hepatocyte plasma membrane. *J Biol Chem* **270:** 1074–1081, 1995.
54. Kamp F, Zakim D, Zhang F, Noy N and Hamilton JA, Fatty acid flip-flop in phospholipid bilayers is extremely fast. *Biochemistry* **34:** 11928–11937, 1995.
55. Tewey KM, Rowe TC, Yang L, Halligan BD and Liu LF, Adriamycin-induced DNA damage mediated by mammalian DNA-topoisomerase II. *Science* **226:** 466–468, 1984.
56. Friche E, Danks MK, Schmidt CA and Beck WT, Decreased DNA topoisomerase II in daunorubicin-resistant Ehrlich ascites tumor cells. *Cancer Res* **51:** 4213–4218, 1991.
57. Friche E, Danks MK and Beck WT, Characterization of tumor cell resistance to 4′-deoxy-4′-iododoxorubicin developed in Ehrlich ascites cells *in vivo*. *Cancer Res* **52:** 5701–5706, 1992.
58. Menozzi M, Valentini L, Vannini E and Arcamone F, Self-association of doxorubicin and related compounds in aqueous solution. *J Pharm Sci* **73:** 766–770, 1984.